

1 **An antisense RNA capable of modulating the
2 expression of the tumor suppressor microRNA-34a**
3

4 **Jason T. Serviss^{1*}, Felix Clemens Richter^{1,2}, Nathanael Johansson
5 Andrews¹, Miranda Houtman, Laura Schwarzmüller, Per Johnsson,
6 Jimmy Van Den Eynden, Erik Larsson³, Dan Grandér¹, Katja Pokrovskaia
7 Tamm¹**

8
9 ¹ Department of Oncology and Pathology, Karolinska Institutet, Stockholm,
10 Sweden

11 ² Kennedy Institute of Rheumatology, University of Oxford, Roosevelt Drive,
12 Oxford OX3 7FY, UK

13 ³Department of Medical Biochemistry and Cell Biology, Institute of
14 Biomedicine, The Sahlgrenska Academy, University of Gothenburg, SE-405
15 30 Gothenburg, Sweden

16 *** Correspondence:**

17 Jason T. Serviss, Department of Oncology and Pathology, Karolinska
18 Institutet, Stockholm, Sweden, SE-17177. jason.serviss@ki.se

22 **Abstract**

23 Long non-coding RNAs transcribed in an antisense orientation to sense
24 protein-coding genes have been increasingly shown to play pivotal roles in
25 regulating gene expression in both *cis* and *trans*. Expression of these
26 antisense transcripts has often been shown to be dys-regulated in cancer
27 giving rise to an altered expression of the corresponding sense gene. Here we
28 describe the ability of a human antisense RNA to regulate levels of
29 the *miR34a* tumor suppressor gene. *miR34a* is a downstream target
30 of *TP53* and mediates critical cellular functions such as cellular growth and
31 senescence. We find that the *miR34a* antisense RNA, a long non-coding RNA
32 transcribed antisense to *miR34a*, is critical for *miR34a* expression and
33 mediation of its cellular functions.

34
35
36

37 **Introduction**

38 In recent years advances in functional genomics has revolutionized our
39 understanding of the human genome. Evidence now points to the fact that
40 approximately 75% of the genome is transcribed but only ~1.2% of this is
41 responsible for encoding proteins (International Human Genome Sequencing
42 2004, Djebali et al. 2012). The newly discovered non-coding elements have
43 been categorized dependent on their function, size, localization, and
44 orientation although a strict definition of these categories is an ongoing
45 process. Of these recently identified elements, long non-coding (lnc) RNAs
46 are defined as transcripts exceeding 200bp in length with a lack of a
47 functional open reading frame. lncRNAs tend to exhibit increased tissue
48 specificity, decreased expression levels, and less conservation than protein
49 coding genes (Derrien et al. 2012). The vast prevalence of transcribed
50 lncRNAs throughout the genome originally led to the speculation that these
51 transcripts were non-functional “transcriptional relics” although further
52 investigation has found lncRNAs to have important regulatory functions in
53 processes such as development, cell fate, and oncogenesis (Rinn et al. 2007,
54 Struhl 2007, Yap et al. 2010). Although many lncRNAs have been identified,
55 the majority still have an unknown biological role and are yet to be functionally
56 characterized (Derrien et al. 2012).

57

58 Some lncRNAs are dually classified as antisense (as) RNAs that are
59 expressed from the same locus as a sense transcript in an antisense
60 orientation. The phenomenon of asRNA transcription has been described in a
61 large variety of eukaryotic organisms and was first discovered long before the

62 advent of modern sequencing technologies (Wagner et al. 1994, Vanhee-
63 Brossollet et al. 1998). With new high-throughput transcriptome sequencing,
64 current estimates indicate that up to 20-40% of the estimated 20,000 protein-
65 coding genes exhibit antisense transcription (Chen et al. 2004, Katayama et
66 al. 2005, Ozsolak et al. 2010). asRNAs have been shown to be expressed in
67 both a concordant and discordant fashion with their sense transcript and can
68 arise from independent promoters, bi-directional promoters exhibiting
69 divergent transcription, as well as cryptic promoters (Core et al. 2008, Seila et
70 al. 2008, Neil et al. 2009, Sigova et al. 2013). Examples of asRNA-mediated
71 gene regulation are becoming increasingly prevalent and are often, but not
72 exclusively, mediated in *cis* resulting in the modulation of sense gene levels.
73 The mechanisms by which they accomplish this are largely diverse stretching
74 from recruitment of chromatin modifying factors (Rinn et al. 2007), acting as
75 microRNA (miRNA) sponges (Memczak et al. 2013), and causing
76 transcriptional interference (Conley et al. 2012).

77

78 The hypothesis that asRNAs play an important role in oncogenesis was first
79 proposed when studies increasingly found examples of aberrant expression of
80 these transcripts and other lncRNA subgroups in tumor samples (Balbin et al.
81 2015). Functional characterization of individual transcripts led to the discovery
82 of asRNA-mediated regulation of several known tumorigenic factors. For
83 example, the asRNA ANRIL was found to be up-regulated in leukemia and to
84 function by repressing CDKN2B, an important regulator of cell cycle G1
85 progression (Yap et al. 2010). Furthermore, the tumor suppressor PTEN has
86 been shown to be regulated both transcriptionally and post-transcriptionally by

87 asRNA transcripts (Johnsson et al. 2013). In addition, the
88 asRNA *HOTAIR* has been shown to negatively regulate the *HOXD* locus via
89 recruitment of Polycomb Repressive Complex 2 mediating epigenetic
90 silencing (Rinn et al. 2007). Although studies characterizing the functional
91 importance of asRNAs in cancer are limited to date, it is becoming
92 increasingly apparent that they play critical roles in regulating key cancer
93 initiation and progression pathways; reviewed in (Spizzo et al. 2012).

94

95 Responses to cellular stress, e.g. DNA damage, sustained oncogene
96 expression, and nutrient deprivation, are all tightly monitored and orchestrated
97 cellular pathways that are commonly dys-regulated in cancer. Cellular
98 signaling in response to these types of cellular stress often converge on the
99 transcription factor *TP53* that regulates transcription of coding and non-coding
100 downstream targets. One non-coding target of *TP53* is the tumor suppressor
101 microRNA known as *miR34a* (Raver-Shapira et al. 2007).
102 Upon *TP53* activation *miR34a* expression is increased allowing it to down-
103 regulate its targets involved in cellular pathways such as, growth factor
104 signaling, apoptosis, differentiation, and cellular senescence (Lal et al. 2011,
105 Slabakova et al. 2017). *miR34a* is a crucial factor in mediating activated *TP53*
106 response and it is often deleted or down-regulated in human cancers and has
107 also been shown to be a valuable prognostic marker (Cole et al. 2008,
108 Gallardo et al. 2009, Zenz et al. 2009, Cheng et al. 2010, Liu et al. 2011).
109 Reduced *miR34a* transcription has been shown to be mediated via epigenetic
110 regulation in many solid tumors, such as colorectal-, pancreatic-, and ovarian
111 cancer (Vogt et al. 2011), as well as multiple types of hematological

112 malignancies (Chim et al. 2010). In addition, miR34a has been shown to be
113 transcriptionally regulated via TP53 homologs, TP63 and TP73, other
114 transcription factors, e.g. STAT3 and MYC, and, in addition, post-
115 transcriptionally through miRNA sponging by the NEAT1 lncRNA (Chang et al.
116 2008, Su et al. 2010, Agostini et al. 2011, Rokavec et al. 2015, Ding et al.
117 2017). Despite these findings, the mechanisms underlying miR34a regulation
118 in the context of oncogenesis have not yet been fully elucidated.

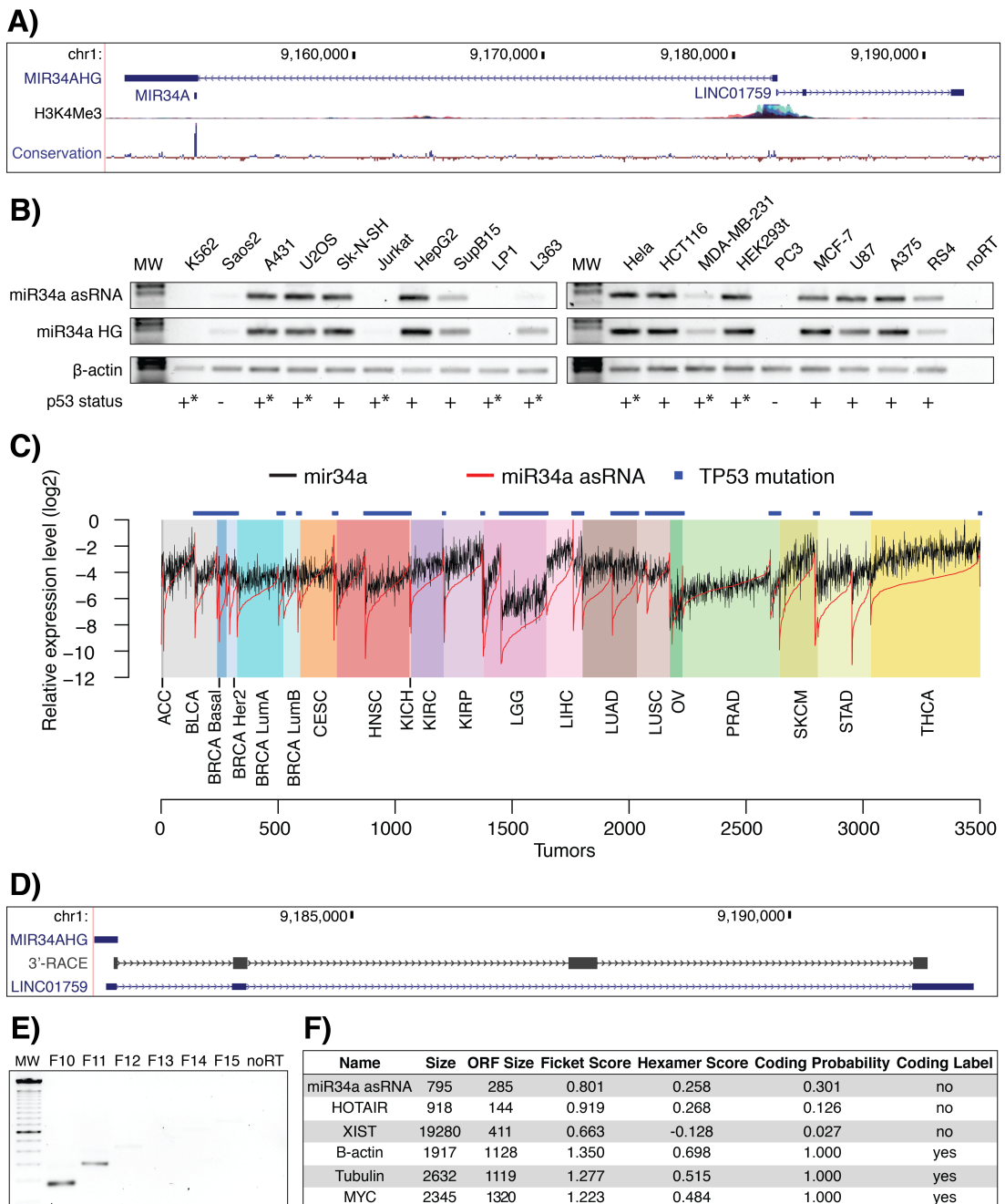
119

120 Multiple studies across different cancers have reported a decrease in
121 oncogenic phenotypes when miR34a expression is induced in a p53-null
122 background, although endogenous mechanisms for achieving this have not
123 yet been discovered (Liu et al. 2011, Ahn et al. 2012, Yang et al. 2012,
124 Stahlhut et al. 2015, Wang et al. 2015). In addition, previous reports have
125 identified a lncRNA originating in the antisense orientation from the miR34a
126 locus which is regulated by TP53 and is induced upon cellular stress (Rashi-
127 Elkeles et al. 2014, Hunten et al. 2015, Leveille et al. 2015, Ashouri et al.
128 2016, Kim et al. 2017). Despite this, none of these studies have continued to
129 functionally characterize this transcript. In this study we functionally
130 characterize the *miR34a* asRNA transcript, finding that modulating the levels
131 of the *miR34a* asRNA is sufficient to increase levels of *miR34a* and results in
132 a decrease of multiple tumorigenic phenotypes. Furthermore, we find that
133 miR34a asRNA-mediated up-regulation of miR34a is sufficient to induce
134 endogenous cellular mechanisms counteracting several types of stress stimuli
135 in a TP53 deficient background.

136

137 **Results**

138
139 **Characterization of the *miR34a* asRNA transcript**
140
141 In order to evaluate possible asRNA-mediated regulation of miR34a
142 expression, we began by examining evidence for asRNA transcripts at the
143 miR34a locus. This revealed an annotated lncRNA (*LINC01759*, also known
144 as *RP3-510D11.2*) transcript in a “head-to-head” orientation with
145 approximately 100 base pair overlap with the *miR34a* HG, hereafter referred
146 to as miR34a asRNA (Fig. 1a). Sentence about conservation and H3K4 at
147 locus? Due to the fact that sense/antisense pairs can be either concordantly
148 or discordantly expressed we next sought to evaluate this relationship in the
149 case of *miR34a* HG and asRNA. Using a diverse panel of cancer cell lines,
150 we were able to detect co-expression of both the *miR34a* HG
151 and *miR34a* asRNA (Fig. 1b). We included *TP53*+/+, *TP53*
152 mutated, and *TP53*-/ cell lines in the panel due to previous reports
153 that *miR34a* is a known downstream target of *TP53*. These results indicate
154 that *miR34a* HG and *miR34a* asRNA are co-expressed and that their
155 expression levels correlate with *TP53* status, with *TP53*+/+ cell lines tending
156 to have higher expression of both transcripts.



157

158 **Figure 1: Characterization of the miR34a asRNA transcript.** A) A schematic picture of
159 the miR34a locus from UCSC genome browser (hg38) including mature miR34a, and
160 LINC01759. H3K4me3 ChIP-seq data and conservation over the locus is also shown. B)
161 Semi-quantitative PCR data from the screening of a panel of cancer cell lines. * Indicates wild-
162 type TP53 with mechanisms present, which inhibit TP53 function (such as SV40 large T antigen in the
163 case of HEK293T cells). C) A graphical depiction of the TCGA correlation analysis. The TP53 mutated
164 samples only include non-synonymous TP53 mutations. Adrenocortical carcinoma (ACC), Bladder
165 Urothelial Carcinoma (BLCA), Breast invasive carcinoma (BRCA), Head and Neck squamous cell
166 carcinoma (HNSC), Kidney Chromophobe (KICH), Lower Grade Glioma (LGG), Liver hepatocellular
167 carcinoma (LIHC), Ovarian serous cystadenocarcinoma (OV), Prostate adenocarcinoma (PRAD), Skin
168 Cutaneous Melanoma (SKCM), Stomach adenocarcinoma (STAD). D) 3'-RACE sequencing results
169 together with the annotated miR34a asRNA (LINC01759). E) Semi-quantitative PCR results from the
170 primer walk assay performed using HEK293T cells. F) Coding potential analysis assessed using the
171 Coding-potential Assessment Tool including miR34a asRNA and two characterized lncRNA transcripts
172 (HOATIR and XIST) and three known protein coding transcripts (β -actin, tubulin, and MYC).

173

174 We next sought to interrogate primary cancer samples to examine if a
175 correlation between *miR34a* asRNA and *miR34a* expression levels could be
176 identified. For this task we utilized RNA sequencing data from The Cancer
177 Genome Atlas (TCGA) after stratifying patients by cancer type, *TP53* status
178 and, in select cases, cancer subtypes. The results indicate
179 that *miR34a* asRNA and *miR34a* expression are strongly correlated in the
180 vast majority of cancer types examined, both in the presence and absence of
181 wild-type *TP53* (**Fig. 1c, Supplementary Fig. 1a**). The results also further
182 confirm that the expression of both *miR34a* and its asRNA have a tendency to
183 be reduced in patients with non-synonymous *TP53* mutations.

184

185 Next, we aimed to gain a thorough understanding of *miR34a* asRNA's
186 molecular characteristics and cellular localization. Polyadenylation status was
187 evaluated via cDNA synthesis with either random nanomers or oligoDT
188 primers followed by semi-quantitative PCR with results indicating that
189 the *miR34a* asRNA is polyadenylated although the unspliced form seems to
190 only be in the polyA negative state (**Supplementary Fig. 1c**). To
191 experimentally determine the 3' termination site for the *miR34a* asRNA
192 transcript we performed 3' rapid amplification of cDNA ends (RACE) using the
193 U2OS osteosarcoma cell line that exhibited high endogenous levels
194 of *miR34a* asRNA in the cell panel screening. Sequencing of the resulting
195 cloned cDNA indicated the transcripts 3' transcription termination site to be
196 525 base pairs upstream of the *LINC01759* transcript's annotated termination
197 site (**Fig. 1d**). Next, we characterized the *miR34a* asRNA 5' transcription start
198 site by carrying out a primer walk assay. A common reverse primer was

199 placed in exon 2 and forward primers were gradually staggered upstream of
200 the transcripts annotated start site (**Supplementary Fig. 1b**). Our results
201 indicated that the 5' start site for *miR34a* asRNA is in fact approximately 90bp
202 (F11 primer) to 220bp (F12 primer) upstream of the annotated start site (**Fig.**
203 **1e**). We furthermore investigated the propensity of *miR34a* asRNA to be
204 alternatively spliced, using PCR cloning and sequencing and found that the
205 transcript is post-transcriptionally spliced to form multiple different isoforms
206 (**Supplementary Fig. 1d**). *make an additional supplementary figure showing
207 spliced RNAseq reads* Finally, to evaluate the cellular localization of miR34a
208 asRNA we utilized RNA sequencing data from five cancer cell lines included
209 in the ENCODE (Consortium 2012) project that had been fractionated into
210 cytosolic and nuclear fractions. The analysis revealed that the *miR34a* asRNA
211 transcript localizes to both the nucleus and cytoplasm but primarily resides in
212 the nucleus (**Supplementary Fig. 1f**).

213

214 Finally, we utilized multiple approaches to evaluate the coding potential of
215 the *miR34a* asRNA transcript. The Coding-Potential Assessment Tool is a
216 bioinformatics-based tool that uses a logistic regression model to evaluate
217 coding-potential by examining ORF length, ORF coverage, Fickett score and
218 hexamer score (Wang et al. 2013). Results indicated that *miR34a* asRNA has
219 a similar lack of coding capacity to the known non-coding
220 transcripts *HOTAIR* and *XIST* and differs greatly when examining these
221 parameters to the known coding transcripts β -actin, tubulin, and *MYC* (**Fig.**
222 **1F**). We further confirmed these results using the Coding-Potential Calculator
223 that utilizes a support based machine-based classifier and accesses an

224 alternate set of discriminatory features (**Supplementary Fig. 1E**) (Kong et al.
225 2007). *To fully evaluate coding potential methods such as mass
226 spectrometry or ribosome profiling must be used, however *miR34a* asRNA
227 presents little evidence of coding potential as evaluated by these two
228 bioinformatic approaches (31) [31]. We hope to be able to scan for peptides
229 matching to *miR34a* asRNA in TCGA before submission and, instead, will
230 mention results here....*

231

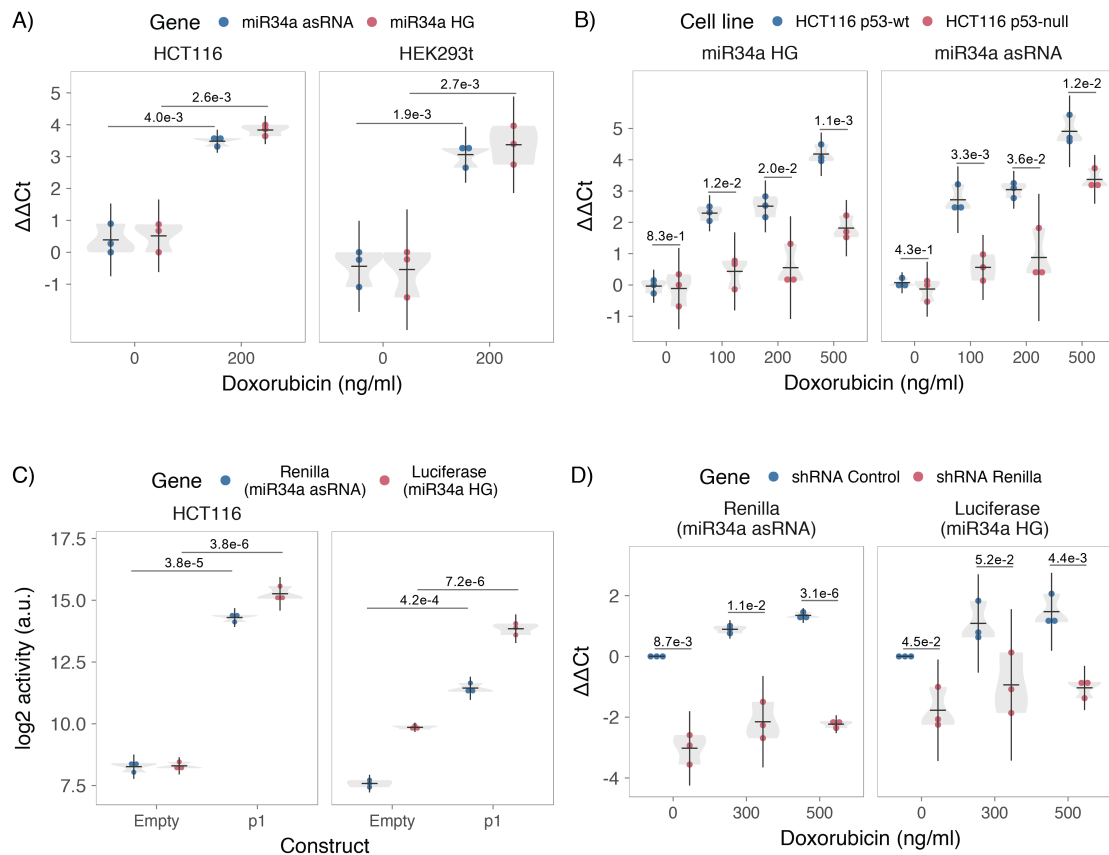
232 ***TP53*-mediated regulation of *miR34a* asRNA expression**

233 *miR34a* is a known downstream target of *TP53* and has been previously
234 shown to exhibit increased expression within multiple contexts of cellular
235 stress. Due to the strong correlation between *miR34a* and *miR34a* asRNA
236 expression, we hypothesized that *miR34a* asRNA may be regulated in a
237 similar fashion whereby transcription is stimulated by the activation of *TP53*.
238 To test this, we treated HEK293t, embryonic kidney cells, and HCT116,
239 colorectal cancer cells, with the DNA damaging agent doxorubicin to activate
240 *TP53*. QPCR-mediated measurement of both *miR34a* HG and asRNA
241 indicated that their expression levels were increased in response to
242 doxorubicin treatment in both cell lines (**Fig. 2a**). This result corresponds well
243 with previous reports of *miR34a* asRNA response in other biological contexts
244 (Rashi-Elkeles et al. 2014, Hunten et al. 2015, Leveille et al. 2015, Ashouri et
245 al. 2016, Kim et al. 2017). To access if it is in fact *TP53* that is responsible for
246 the increase in *miR34a* asRNA expression upon DNA damage, we
247 treated *TP53*^{+/+} and *TP53*^{-/-} HCT116 cells with increasing concentrations of the
248 doxorubicin and monitored the expression of both *miR34a* HG and asRNA.

249 We observed a dose-dependent increase in both *miR34a* HG and asRNA
250 expression levels with increasing amounts of doxorubicin, indicating that
251 these two transcripts are co-regulated, although, this effect was largely
252 abrogated in *TP53*^{-/-} cells (**Fig. 2b**). These results indicate
253 that *TP53* activation increases *miR34a* asRNA expression upon the induction
254 of DNA damage. Despite this, *TP53*^{-/-} cells also showed a dose dependent
255 increase in both *miR34a* HG and asRNA, indicating that additional factors,
256 other than *TP53*, are capable of initiating an increase in expression of both of
257 these transcripts upon DNA damage.

258

259



260 **Figure 2: TP53-mediated regulation of the *miR34a* locus.** **A)** Evaluating the effects of 24 hours of
261 treatment with 200 ng/ml doxorubicin on *miR34a*asRNA and HG in HCT116 and HEK293t
262 cells.* **B)** Monitoring *miR34a* HG and asRNA expression levels during 24 hours doxorubicin treatment
263 in *TP53*^{+/+} and *TP53*^{-/-} HCT116 cells.* **C)** Quantification of luciferase and renilla levels after
264 transfection of HCT116 and HEK293T cells with the p1 construct.* **D)** HCT116 cells were co-
265 transfected with the p1 construct and shRNA renilla or shRNA control and subsequently treated with
266 increasing doses of doxorubicin. 24 hours post-treatment, cells were harvested and renilla and
267 luciferase levels were measured using QPCR. Resulting p-values from statistical testing are shown
268 above the shRenilla samples which were compared to the shRNA control using the respective treatment
269 condition.* *Individual points represent results from independent experiments and the gray shadow
270 indicates the density of those points. Error bars show the 95% CI, black horizontal lines represent the
271 mean, and p-values are shown over long horizontal lines indicating the comparison tested.
272

273 It is likely, due to the head-to head orientation of *miR34a* HG and asRNA, that
274 transcription may be initiated from a single promoter in a bi-directional
275 manner. To investigate whether *miR34a* HG and asRNA are transcribed from
276 the same promoter as divergent transcripts, we cloned the *miR34a* HG
277 promoter, including the *TP53* binding site, into a luciferase/renilla dual
278 reporter vector which we hereafter refer to as p1 (**Supplementary Fig. 2a**
279 **and 2b**). Upon transfection of p1 into HCT116 and HEK293t cell lines we
280 observed increases in both luciferase and renilla indicating that *miR34a* HG
281 and asRNA expression can be regulated by a single promoter contained
282 within the p1 construct (**Fig. 2c**).

283

284 Functional characterization of individual antisense transcripts has previously
285 shown their capability to regulate their sense gene (Yap et al. 2010,
286 Pelechano et al. 2013). We therefore investigated the possibility
287 that *miR34a* asRNA may regulate *miR34a* HG levels. We hypothesized that
288 the overlapping regions of the sense and antisense transcripts may have a
289 crucial role in *miR34a* asRNAs ability to regulate *miR34a* HG, possibly via
290 RNA:DNA or RNA:RNA interaction. Accordingly, we first co-transfected the p1
291 construct, containing the overlapping region of the two transcripts, and a short
292 hairpin (sh) RNA targeting renilla into HCT116 cells subsequently treating
293 them with increasing doses doxorubicin. Analysis of luciferase and renilla
294 expression revealed that shRNA-mediated knock down of the renilla transcript
295 (corresponding to *miR34a* asRNA) caused luciferase (corresponding
296 to *miR34a* HG) levels to concomitantly decrease (**Fig. 2d**). Collectively, these
297 results indicate that *miR34a* asRNA positively regulates levels of *miR34a* HG

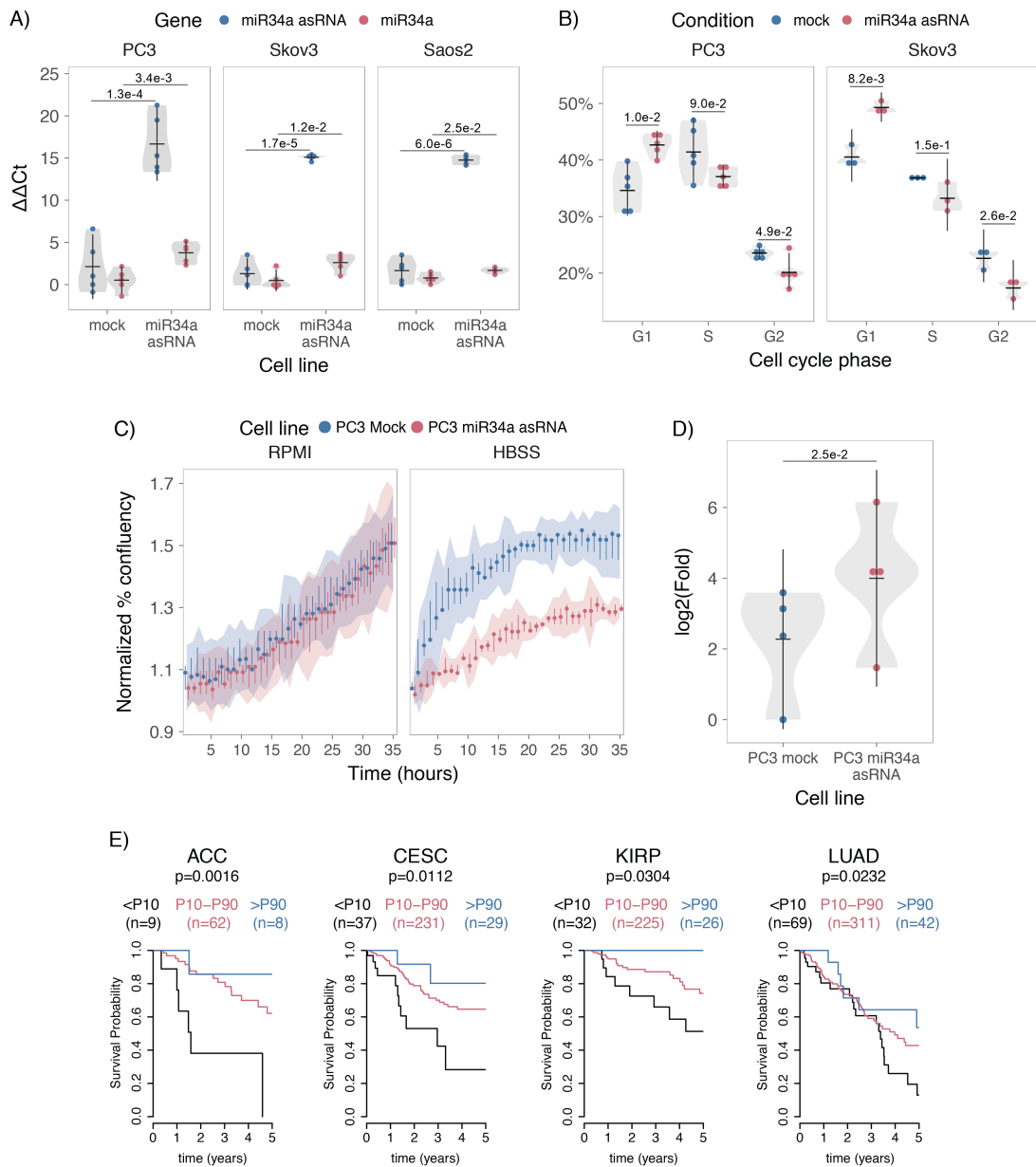
298 and is crucial for an appropriate TP53-mediated *miR34a* response to DNA
299 damage.

300

301 **Functional analysis of *miR34a* asRNA in *TP53*-deficient cells**

302 Despite the fact that *TP53* regulates *miR34a* HG and asRNA expression, our
303 results indicated that other factors are also able to regulate this locus (**Fig.**
304 **2b**). Utilizing a lentiviral system, we stably over-expressed the *miR34a* asRNA
305 transcript in three *TP53*-null cell lines; PC3 (prostate cancer), Saos2
306 (osteogenic sarcoma), and Skov3 (adenocarcinoma). We first analyzed the
307 levels of *miR34a* asRNA in these stable over-expression cell lines, compared
308 to HEK293T cells, which have high endogenous levels of *miR34a* asRNA,
309 finding that, on average, the over-expression was approximately 30-fold
310 higher in the over-expression cell lines than in HEK293t cells. Due to the fact
311 that *miR34a* asRNA can be up-regulated ~30-fold in response to DNA
312 damage (**Fig. 2b**), we deemed this over-expression level to correspond to
313 physiologically relevant levels in cells encountering a stress stimulus, such as
314 DNA damage (**Supplementary Fig. 3a**). Analysis of *miR34a* levels in
315 the *miR34a* asRNA over-expressing cell lines showed that *miR34a* asRNA
316 over-expression resulted in a concomitant increase in the expression
317 of *miR34a* in all three cell lines (**Fig. 3a**). These results indicate that, in the
318 absence of TP53, *miR34a* expression may be rescued by increasing the
319 levels of *miR34a* asRNA expression.

320



321 **Figure 3: miR34a asRNA positively regulates miR34a and its associated phenotypes.** A) QPCR-
322 mediated quantification of miR34a expression in cell lines stably over-
323 expressing miR34a asRNA.* B) Cell cycle analysis comparing stably over-expressing miR34a asRNA
324 cells to the respective mock expressing cells.* C) Analysis of cellular growth over time in miR34a
325 asRNA over-expressing PC3 cells. Points represent the median from 3 independent experiments and
326 the colored shadows indicate the 95% confidence interval. D) Differential phosphorylated polymerase
327 II binding in miR34a asRNA over-expressing PC3 cells.* E) Survival analysis dependent
328 on miR34a asRNA expression levels using TCGA data. P10 = 10%, P10-P90 = 10%-90%, P90 = 90%.
329 Adrenocortical carcinoma (ACC), Cervical squamous cell carcinoma and endocervical adenocarcinoma
330 (CESC), Kidney renal papillary cell carcinoma (KIRP), Lung adenocarcinoma (LUAD). *Individual
331 points represent results from independent experiments and the gray shadow indicates the density of
332 those points. Error bars show the 95% CI, black horizontal lines represent the mean, and p-values are
333 shown over long horizontal lines indicating the comparison tested.
334

335 *miR34a* has been previously shown to regulate cell cycle progression, with
336 increasing levels of *miR34a* causing senescence via G1 arrest. Cell cycle
337 analysis via determination of DNA content showed a significant increase in G1
338 phase cells in the PC3 and Skov3 *miR34a* asRNA over-expressing cell lines,
339 indicative of G1 arrest, as well as, a significant decrease of cells in G2 phase
340 (**Fig. 3b**). *miR34a*'s effects on the cell cycle are mediated by its ability to
341 target cell cycle regulators such as cyclin D1 (*CCND1*) (Sun et al. 2008). We
342 therefore sought to determine if the *miR34a* asRNA over-expressing cell lines
343 exhibited effects on these known *miR34a* targets. Quantification of
344 both *CCND1* RNA expression (**Supplementary Fig. 3b**) and protein levels
345 (**Supplementary Fig. 3c**) in the PC3 *miR34a* asRNA over-expressing cell line
346 showed a significant decrease of *CCND1* levels in *miR34a* asRNA over-
347 expressing cell lines compared to the mock control.

348

349 *miR34a* is also a well known inhibitor of cellular growth via its ability to
350 regulate growth factor signaling. Furthermore, starvation has been shown to
351 induce *miR34a* expression that down-regulates multiple targets that aid in the
352 phosphorylation of multiple pro-survival and growth factors (Lal et al. 2011).
353 We further interrogated the effects of *miR34a* asRNA over-expression by
354 investigating the growth rate of the cells in both normal and starvation
355 conditions by measuring confluence over a 35-hour period. Although under
356 normal growth conditions there is only a marginal trend towards decreased
357 growth at individual early time points in *miR34a* asRNA over-expressing cell
358 lines, these effects on cell growth are drastically increased in starvation
359 conditions. This is in accordance with our previous results, indicating

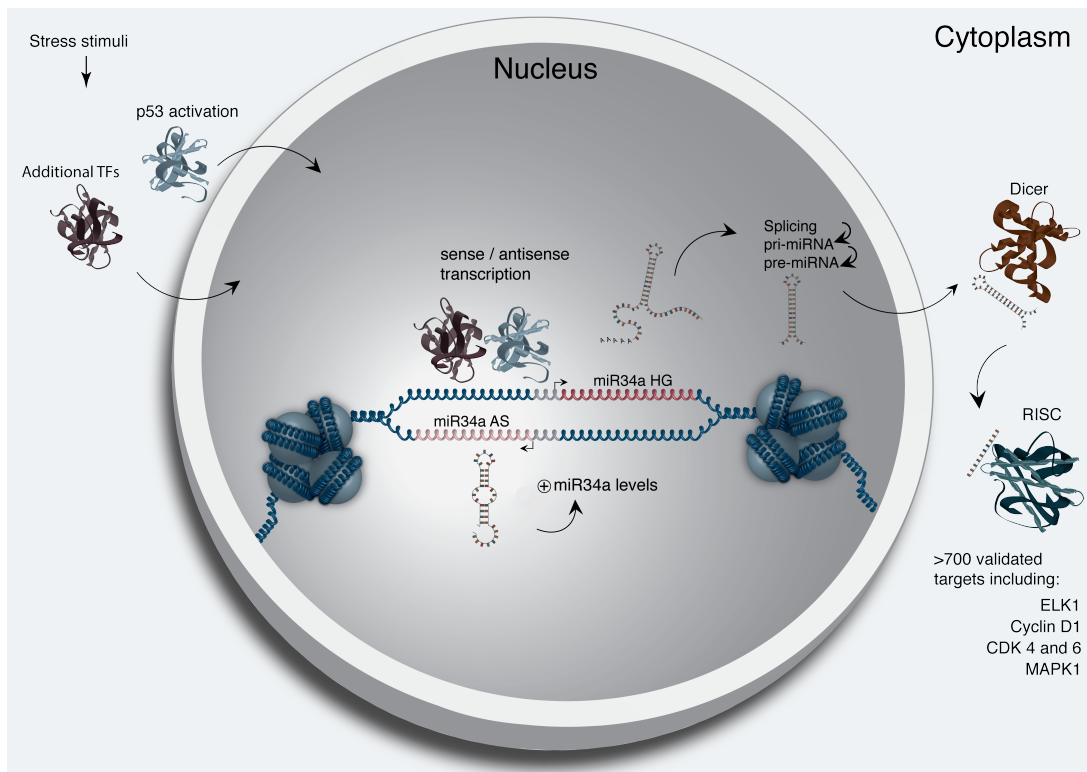
360 that, *miR34a* asRNA-mediated increases in *miR34a* expression are especially
361 crucial under conditions of stress and necessary for the initiation of an
362 appropriate cellular response. In summary, we find that over-expression
363 of *miR34a* asRNA is sufficient to increase *miR34a* expression and gives rise
364 to known phenotypes observed with increased *miR34a* expression.

365

366 Antisense RNAs have been reported to mediate their effects both via
367 transcriptional and post-transcriptional mechanisms. Due to the fact that
368 *miR34a* expression is undetected in wild type PC3 cells but, upon over-
369 expression of *miR34a* asRNA, increases to detectable levels, we
370 hypothesized that *miR34a* asRNA is capable of regulating *miR34a* expression
371 levels via transcriptional mechanisms. To ascertain if this is actually the case,
372 we performed chromatin immunoprecipitation (ChIP) for phosphorylated
373 polymerase II (polII) at the *miR34a* HG promoter in both *miR34a* asRNA over-
374 expressing and mock control cell lines. Our results indicated a clear increase
375 in phosphorylated polII binding at the *miR34a* promoter upon *miR34a* asRNA
376 over-expression indicating *miR34a* asRNA's ability to regulate *miR34a* levels
377 on a transcriptional level (**Fig. 3d**).

378

379 *Finally, we investigated if *miR34a* asRNA levels affected the survival of
380 patients across a broad range of cancer types within the TCGA study. Of the
381 cancer types examined, we identified four where increased *miR34a* asRNA
382 levels gave rise to a beneficial prognosis (**Fig 3g**). This figure will either be
383 removed or modified before submission*



384

385 **Figure 4: A graphical summary of the proposed *miR34a* asRNA function.** Stress stimuli,
 386 originating in the cytoplasm or nucleus, activates *TP53* as well as additional factors. These factors then
 387 bind to the *miR34a* promoter and drive transcription of the sense and antisense strands. *miR34a* asRNA
 388 serves to increase the levels of *miR34a* HG transcription via an unknown mechanism. *miR34a* HG
 389 then, in turn, is then spliced, processed by the RNase III enzyme Drosha, and exported to the
 390 cytoplasm. The *miR34a* pre-miRNA then binds to Dicer where the hair-pin loop is cleaved and
 391 mature *miR34a* is formed. Binding of the mature *miR34a* miRNA to the RISC complex then allows it
 392 to bind and repress its targets.
 393

394 **Discussion**

395
396 Multiple studies have previously shown asRNAs to be crucial for the
397 appropriate regulation of cancer-associated protein-coding genes and that
398 their dys-regulation can lead to perturbation of tumor suppressive and
399 oncogenic pathways, as well as, cancer-related phenotypes. Here we show
400 that asRNAs are also capable of regulating cancer-associated miRNAs
401 resulting in similar consequences as protein-coding gene dys-regulation (**Fig.**
402 **4**). Interestingly, we show that, both in the presence and absence of
403 *TP53*, *miR34a* asRNA provides an additional regulatory level and functions by
404 mediating the increase of *miR34a* expression in both homeostasis and upon
405 encountering multiple forms of cellular stress. Furthermore, we find that
406 *miR34a* asRNA-mediated increases in *miR34a* expression levels are sufficient
407 to drive the appropriate cellular responses to the forms of stress stimuli that
408 are encountered. These results are also supported by others who have
409 utilized various molecular biology methods to up regulate *miR34a* expression
410 in a *p53* deficient background (Liu et al. 2011, Ahn et al. 2012, Yang et al.
411 2012, Stahlhut et al. 2015, Wang et al. 2015).

412

413 In agreement with previous studies, we demonstrate that upon encountering
414 various types of cellular stress, *TP53* in concert with additional factors bind
415 and initiate transcription at the *miR34a* locus, thus increasing the levels of
416 *miR34a* and, in addition, *miR34a* asRNA. We hypothesize that *miR34a*
417 asRNA may form a positive feedback for *miR34a* expression whereby *miR34a*
418 asRNA serves as a scaffold for the recruitment of additional factors that
419 support the expression of *miR34a* and, thus, driving the cell towards a

420 reduction in growth factor signaling, senescence, and eventually apoptosis.
421 On the other hand, in cells without a functional p53, other factors, which
422 typically act independently or in concert with *TP53*, may initiate transcription
423 of the *miR34a* locus. We believe that *miR34a* asRNA could potentially be
424 interacting directly with one of these additional factors and recruiting it to the
425 *miR34a* locus in order to drive *miR34a* transcription. This is especially
426 plausible due to the fact that, due to the head-to-head orientation of the
427 *miR34a* HG and asRNA, there is sequence complementarity between the
428 RNA and the promoter DNA, although further work will need to be performed
429 to ascertain if this binding actually takes place. ***add additional eClip data to
430 supplementary and mention here? Incomplete figure attached to mail***

431

432 Despite the fact that the exact mechanism by which the *miR34a* asRNA
433 operates is not elucidated in this study, several pieces of experimental
434 evidence can provide insights concerning this. In both gain- and loss-of-
435 function experiments (**Figure 2d, Figure 3a**) we note that it is the
436 transcriptional product of the *miR34a* asRNA locus that gives rise to the effect
437 on miR34a levels. This precludes the idea that transcription of *miR34a* asRNA
438 may potentially be sufficient to increase the levels of *miR34a* and, instead,
439 mechanisms must be in place which allow the direct or indirect interaction with
440 the *miR34a* asRNA transcript to stimulate miR34a HG transcription.
441 Furthermore, due to the fact that the p1 construct only contains a small
442 portion of the *miR34a* asRNA transcript, it could be the case that this portion
443 is sufficient to give rise to at least a partial *miR34a* inducing response (**Fig 2d,**
444 **Supplementary Fig. 2a-2b**). Further studies may reveal that utilization of only

445 this short oligonucleotide may be sufficient to increase *miR34a* expression
446 levels and thus provide a potential pathway towards oligonucleotide-mediated
447 therapies. In fact, clinical trials utilizing *miR34a* replacement therapy have
448 previously been conducted but, disappointingly, were terminated after adverse
449 side effects of an immunological nature were observed in several of the
450 patients. Although it is not presently clear if these side effects were caused by
451 *miR34a* or the liposomal carrier used to deliver the miRNA, the multitude of
452 evidence indicating *miR34a*'s crucial role in oncogenesis still makes its
453 therapeutic induction a lucrative strategy for patient treatment and needs
454 further investigation.

455

456 An unannotated transcript, *Lnc34a*, arising from the antisense orientation of
457 the *miR34a* locus and with a transcription start site >250 bp upstream of the
458 annotated *miR34a* asRNAs start site, has been previously reported in a study
459 examining colorectal cancer (Wang et al. 2016). Among the findings in Wang
460 et al. the authors discover that *Lnc34a* negatively regulates *miR34a*
461 expression via recruitment of *DNMT3a*, *PHB2*, and *HDAC1* to the *miR34a*
462 promoter. Although the *Lnc34a* and *miR34a* asRNA transcripts share some
463 sequence similarity, we believe them to be separate RNAs that are,
464 potentially, different isoforms of the same gene. Furthermore, we believe
465 that *Lnc34a* may be highly context dependent and potentially only expressed
466 at biologically significant levels in colon cancer stem cells, or other stem-like
467 cells, in agreement with the conclusions drawn in the paper. We thoroughly
468 address our reasons for these beliefs and give appropriate supporting
469 evidence in (**Supplementary Results 4**). The fact that *Lnc34a* and *miR34a*

470 asRNA would appear to have opposing roles in their regulation of *miR34a*
471 further underlines the complexity of the regulation at this locus.

472

473 In summary, our results indicate that *miR34a* asRNA is a vital player in the
474 regulation of *miR34a* and is especially important in contexts where cellular
475 stresses are encountered. Due to the fact that many of these stress stimuli
476 are strongly associated with cancer, we believe *miR34a* asRNA's ability to
477 fine-tune *miR34a* expression levels to be especially crucial in tumorigenesis.

478

479 **Materials and Methods**

480 **Cell culture**

481 All cell lines were cultured at 5% CO₂ and 37° C with HEK293T cells cultured
482 in DMEM high glucose (Hyclone), HCT116 and U2OS cells in McCoy's 5a
483 (Life Technologies), and PC3 cells in RPMI (Hyclone) and 2 mM L-glutamine
484 **add other cell lines**. All growth mediums were supplemented with 10% heat-
485 inactivated FBS and 50 µg/ml of streptomycin and 50 µg/ml of penicillin.

486 **Bioinformatics and Data availability**

488 The USCS genome browser (Kent et al. 2002) was utilized for the
489 bioinformatic evaluation of antisense transcription utilizing the RefSeq
490 (O'Leary et al. 2016) gene annotation track.

491 All raw experimental data, code used for analysis, and supplementary
492 methods are available for review
493 at https://github.com/GranderLab/miR34a_asRNA_project (Serviss 2017) and
494 are provided as an R package. All analysis took place using the R statistical
495 programming language (Team 2017) using multiple external packages that

496 are all documented in the package associated with the article (Wilkins , Chang
497 2014, Wickham 2014, Wickham 2016, Allaire et al. 2017, Arnold 2017,
498 Wickham 2017, Wickham 2017, Wickham 2017, Xiao 2017, Xie 2017). The
499 package facilitates replication of the operating system and package versions
500 used for the original analysis, reproduction of each individual figure included
501 in the article, and easy review of the code used for all steps of the analysis,
502 from raw-data to figure.

503

504 **Coding Potential**

505 Protein-coding capacity was evaluated using the Coding-potential
506 Assessment Tool (Wang et al. 2013) and Coding-potential Calculator (Kong et
507 al. 2007) with default settings. Transcript sequences for use with Coding-
508 potential Assessment Tool were downloaded from the UCSC genome
509 browser using the Ensembl
510 accessions: *HOTAIR* (ENST00000455246), *XIST* (ENST00000429829), β-
511 actin (ENST00000331789), Tubulin (ENST00000427480),
512 and *MYC* (ENST00000377970). Transcript sequences for use with Coding-
513 potential Calculator were downloaded from the UCSC genome browser using
514 the following IDs: *HOTAIR* (uc031qho.1), β-actin (uc003soq.4).

515

516 **shRNAs**

517 shRNA-expressing constructs were cloned into the U6M2 construct using the
518 BgIII and KpnI restriction sites as previously described (Amarzguioui et al.
519 2005) (Amarzguioui et al. 2005). shRNA constructs were transfected using
520 Lipofectamine 2000 or 3000 (Life Technologies). The sequence targeting

521 renilla is as follows: AAT ACA CCG CGC TAC TGG C.

522

523 **Lentiviral particle production, infection, and selection.**

524 Lentivirus production was performed as previously described in (Turner et al.
525 2012). Briefly, HEK293T cells were transfected with viral and expression
526 constructs using Lipofectamine 2000 (Life Technologies), after which viral
527 supernatants were harvested 48 and 72 hours post-transfection. Viral
528 particles were concentrated using PEG-IT solution (Systems Biosciences)
529 according to the manufacturer's recommendations. HEK293T cells were used
530 for virus titration and GFP expression was evaluated 72hrs post-infection via
531 flow cytometry after which TU/ml was calculated.

532

533 **Western Blotting.**

534 Samples were lysed in 50 mM Tris-HCl, pH 7.4, 1% NP-40, 150 mM NaCl, 1
535 mM EDTA, 1% glycerol, 100 µM vanadate, protease inhibitor cocktail and
536 PhosSTOP (Roche Diagnostics GmbH). Lysates were subjected to SDS-
537 PAGE and transferred to PVDF membranes. The proteins were detected by
538 western blot analysis by using an enhanced chemiluminescence system
539 (Western Lightning-ECL, PerkinElmer). Antibodies used were specific
540 for CCND1 (Cell Signaling, cat. no. 2926, 1:1000), and β-actin (Sigma-Aldrich,
541 cat. no. A5441, 1:5000). All western blot quantifications were performed using
542 ImageJ (Schneider et al. 2012).

543

544 **Generation of U6-expressed miR34a AS lentiviral constructs.**

545 The U6 promoter was amplified from the U6M2 cloning plasmid (Amarzguioui

546 et al. 2005) and ligated into the Not1 restriction site of the pHIV7-IMPDH2
547 vector (Turner et al. 2012). miR43a asRNA was PCR amplified and
548 subsequently cloned into the Nhe1 and Pac1 restriction sites in the pHIV7-
549 IMPDH2-U6 plasmid.

550

551 **Promoter activity.**

552 Cells were co-transfected with the renilla/firefly bidirectional promoter
553 construct (Polson et al. 2011) and GFP by using Lipofectamine 2000 (Life
554 Technologies). The expression of GFP and luminescence was measured 24 h
555 post transfection by using the Dual-Glo Luciferase Assay System (Promega)
556 and detected by the GloMax-Multi+ Detection System (Promega). The
557 expression of luminescence was normalized to GFP.

558

559 **Flow Cytometry.**

560 Cells were harvested, centrifuged and, either re-suspended in PBS, 5% FBS
561 and analyzed for GFP expression using the LSRII machine (BD Biosciences).

562

563 **RNA extraction and cDNA synthesis.**

564 For downstream SYBR green applications, RNA was extracted using the
565 RNeasy mini kit (Qiagen) and subsequently treated with DNase (Ambion
566 Turbo DNA-free, Life Technologies). 500ng RNA was used for cDNA
567 synthesis using MuMLV (Life Technologies) and a 1:1 mix of oligo(dT) and
568 random nanomers.

569 For analysis of miRNA expression with Taqman, samples were isolated with
570 trizol (Life Technologies) and further processed with the miRNeasy kit

571 (Qiagen). cDNA synthesis was performed using the TaqMan MicroRNA
572 Reverse Transcription Kit (Life Technologies) using the corresponding oligos
573 according to the manufacturer's recommendations.

574

575 **QPCR and PCR.**

576 PCR was performed using the KAPA2G fast mix (Kapa Biosystems) with
577 corresponding primers. QPCR was carried out using KAPA 2G SYBRGreen
578 (Kapa Biosystems) using the Applied Biosystems 7900HT machine with the
579 cycling conditions: 95 °C for 3 min, 95 °C for 3 s, 60 °C for 30 s.

580 QPCR for miRNA expression analysis was performed according to the
581 protocol for the TaqMan microRNA Assay kit (Life Technologies) with the
582 same cycling scheme as above. Primer and probe sets for TaqMan were also
583 purchased from Life Technologies (TaqMan® MicroRNA Assay, hsa-miR-34a,
584 human and Control miRNA Assay, RNU48, human).

585 Primers for all PCR-based experiments are listed in **Supplementary Table 1**.

586

587 **Bi-directional promoter.**

588 The overlapping region (p1) corresponds with the sequence previously
589 published as the TP53 binding site in (Raver-Shapira et al. 2007) which we
590 synthesized and cloned into the pLucRluc construct (Polson et al. 2011).

591

592 **Cell-cycle distribution.**

593 Cells were washed in PBS and fixed in 4% PFA at room temperature
594 overnight. PFA was removed, and cells were re-suspended in 95% EtOH. The
595 samples were then rehydrated in distilled water, stained with DAPI and

596 analyzed by flow cytometry on a LSRII (BD Biosciences) machine. Resulting
597 cell cycle phases were quantified using the ModFit software (Verity Software
598 House).

599

600 **3'-RACE**

601 3'-RACE was performed as described as previously in (Johnsson et al. 2013).
602 Briefly, U2OS cell RNA was polyA-tailed using yeast polyA polymerase after
603 which cDNA was synthesized using oligo(dT) primers. Nested-PCR was
604 performed first using a forward primer in miR34a asRNA exon 1 and a tailed
605 oligo(dT) primer followed by a second PCR using an alternate miR34a asRNA
606 exon 1 primer and a reverse primer binding to the tail of the previously used
607 oligo(dT) primer. PCR products were gel purified and cloned the Strata Clone
608 Kit (Agilent Technologies), and sequenced.

609

610 **ChIP**

611 The ChIP was performed as previously described in (Johnsson et al. 2013)
612 with the following modifications. Cells were crosslinked in 1% formaldehyde,
613 quenched with glycine (0.125M), and lysed in cell lysis buffer (5mM PIPES,
614 85mM KCL, 0.5% NP40, protease inhibitor) and, sonicated in (50mM TRIS-
615 HCL pH 8.0, 10mM EDTA, 1% SDS, protease inhibitor) using a Bioruptor
616 Sonicator (Diagenode). Samples were incubated over night at 4°C with
617 the *polII* antibody (Abcam: ab5095) and subsequently pulled down with
618 Salmon Sperm DNA/Protein A Agarose (Upstate/Millipore) beads. DNA was
619 eluted in Elution buffer (1% SDS, 100mM NaHCO3), followed by reverse
620 crosslinking, RNaseA and protease K treatment. The DNA was eluted using

621 Qiagen PCR purification kit.

622 **Confluency Analysis**

623 **Fill this in**

624 **Pharmacological Compounds**

625 Doxorubicin was purchased from Teva (cat. nr. 021361). Actinomycin D was
626 purchased from Sigma-Aldrich (cat. nr. A1410-2MG).

627

628 **CAGE analysis**

629 All available CAGE data from the ENCODE project (Consortium 2012) for 36
630 cell lines was downloaded from the UCSC genome browser (Kent et al. 2002)
631 for genome version hg19. Of these, 28 cell lines had CAGE transcription start
632 sites (TSS) mapping to the plus strand of chromosome 1 and in regions
633 corresponding to 200 base pairs upstream of the *lnc34a* start site (9241796 -
634 200) and 200 base pairs upstream of the GENCODE
635 annotated *miR34a* asRNA start site (9242263 + 200). These cell lines
636 included: HFDPC, H1-hESC, HMEpC, HAoEC, HPIEpC, HSaVEC, GM12878,
637 hMSC-BM, HUVEC, AG04450, hMSC-UC, IMR90, NHDF, SK-N-SH_RA, BJ,
638 HOB, HPC-PL, HAoAF, NHEK, HVMF, HWP, MCF-7, HepG2, hMSC-AT,
639 NHEM.f_M2, SkMC, NHEM_M2, and HCH. In total 74 samples were included.
640 17 samples were polyA-, 47 samples were polyA+, and 10 samples were total
641 RNA. In addition, 34 samples were whole cell, 15 enriched for the cytosolic
642 fraction, 15 enriched for the nucleolus, and 15 enriched for the nucleus. All
643 CAGE transcription start sites were plotted and the RPKM of the individual
644 reads was used to colour each read to indicate their relative abundance. In
645 cases where CAGE TSS spanned identical regions, the RPMKs of the regions

646 were summed and represented as one CAGE TSS in the figure. In addition, a
647 density plot shows the distribution of the CAGE reads in the specified
648 interval.

649

650 **Splice junction analysis**

651 All available whole cell (i.e. non-fractionated) spliced read data originating
652 from the Cold Spring Harbor Lab in the ENCODE project (Consortium 2012)
653 for 38 cell lines was downloaded from the UCSC genome browser (Kent et al.
654 2002). Of these cell lines, 36 had spliced reads mapping to the plus strand of
655 chromosome 1 and in the region between the *lnc34a* start (9241796) and
656 transcription termination (9257102) site (note that *miR34a* asRNA resides
657 totally within this region). Splice junctions from the following cell lines were
658 included in the final figure: A549, Ag04450, Bj, CD20, CD34 mobilized,
659 Gm12878, H1hesc, Haoaf, Haoec, Hch, Helas3, Hepg2, Hfdpc, Hmec,
660 Hmepc, Hmescat, Hmscbm, Hmscuc, Hob, Hpcpl, Hpiepc, Hsavec, Hsmm,
661 Huvec, Hvmf, Hwp, Imr90, Mcf7, Monocd14, Nhdf, Nhek, Nhemfm2,
662 Nhemm2, Nhlf, Skmc, and Sknsh. All splice junctions were included in the
663 figure and coloured according to the number of reads corresponding to
664 each. In cases where identical reads were detected multiple times, the read
665 count was summed and represented as one read in the figure.

666

667 **Correlation analysis**

668 Erik/Jimmy should probably take this.

669

670 **Acknowledgments**

671

672 **Competing Interests**

673

674 The authors declare no competing interests.

675

676 **Figure Supplements**

677

678 List figure supplements here!

679

680 **Supplementary Figures**

681

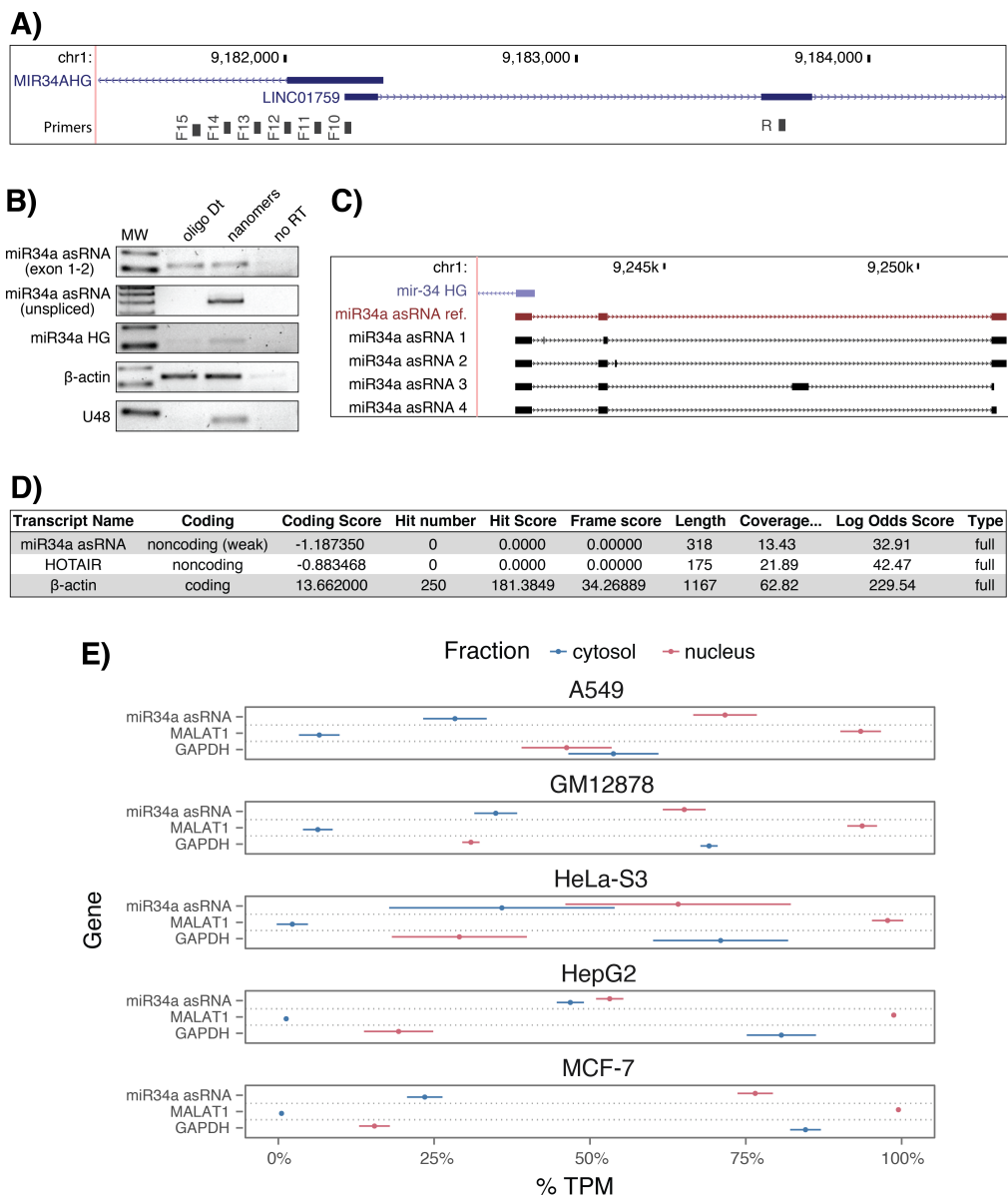
682

A)

cancer	all n	all rho	all p	TP53wt n	TP53wt rho	TP53wt p	TP53mut n	TP53mut rho	TP53mut p
ACC	10	5.52e-01	1.04e-01	10	5.52e-01	1.04e-01	NA	NA	NA
BLCA	228	5.15e-01	7.89e-17	134	4.53e-01	3.86e-08	94	4.27e-01	1.73e-05
BRCA Basal	42	5.74e-01	9.54e-05	10	6.24e-01	6.02e-02	32	5.74e-01	7.41e-04
BRCA Her2	44	1.47e-01	3.39e-01	12	2.24e-01	4.85e-01	32	6.82e-02	7.10e-01
BRCA LumA	199	3.41e-01	8.22e-07	177	3.43e-01	2.96e-06	22	4.86e-01	2.31e-02
BRCA LumB	70	1.71e-01	1.57e-01	61	1.48e-01	2.53e-01	9	1.67e-01	6.78e-01
CESC	156	1.39e-01	8.37e-02	145	1.60e-01	5.45e-02	11	-4.55e-02	9.03e-01
HNSC	313	5.37e-01	8.38e-25	123	6.08e-01	0.00e+00	190	4.47e-01	9.68e-11
KICH	5	6.00e-01	3.50e-01	5	6.00e-01	3.50e-01	NA	NA	NA
KIRC	142	3.49e-01	2.06e-05	141	3.37e-01	4.41e-05	NA	NA	NA
KIRP	167	4.51e-01	9.16e-10	163	4.48e-01	2.04e-09	4	8.00e-01	3.33e-01
LGG	271	6.33e-01	9.92e-32	76	7.28e-01	0.00e+00	195	3.87e-01	2.26e-08
LIHC	153	5.63e-01	3.64e-14	114	5.16e-01	4.18e-09	39	4.55e-01	3.95e-03
LUAD	234	2.82e-01	1.15e-05	128	3.61e-01	2.87e-05	106	2.27e-01	1.91e-02
LUSC	139	2.29e-01	6.74e-03	42	4.17e-02	7.93e-01	97	3.29e-01	9.91e-04
OV	56	2.33e-01	8.37e-02	10	8.42e-01	4.46e-03	46	1.46e-01	3.31e-01
PRAD	413	4.66e-01	1.33e-23	375	4.59e-01	6.13e-21	38	4.50e-01	4.58e-03
SKCM	165	6.48e-01	5.43e-21	152	6.10e-01	7.85e-17	13	4.34e-01	1.40e-01
STAD	225	3.72e-01	8.23e-09	145	3.67e-01	5.71e-06	80	4.20e-01	1.03e-04
THCA	469	4.58e-01	1.07e-25	467	4.62e-01	4.06e-26	NA	NA	NA

683
684
685
686
687
688
689
690
691

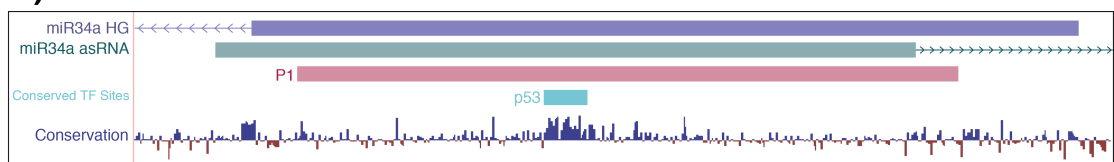
Figure 1_Supplement 1: A) Spearman's rho and p-values (p) from the correlation analysis investigating the correlation between miR34a and miR34a asRNA expression in TP53 wild type (wt) and mutated (mut) samples within TCGA cancer types. Bladder Urothelial Carcinoma (BLCA), Breast invasive carcinoma (BRCA), Head and Neck squamous cell carcinoma (HNSC), Lower Grade Glioma (LGG), Liver hepatocellular carcinoma (LIHC), Lung adenocarcinoma (LUAD), Lung squamous cell carcinoma (LUSC), Ovarian serous cystadenocarcinoma (OV), Prostate adenocarcinoma (PRAD), Skin Cutaneous Melanoma (SKCM), Stomach adenocarcinoma (STAD).



692
693
694
695
696
697
698
699
700
701
702
703

Figure 1 Supplement 2: **A)** A schematic representation of the primer placement in the primer walk assay. **B)** Polyadenylation status of spliced and unspliced miR34a asRNA in HEK293T cells. **C)** Sequencing results from the analysis of *miR34a* asRNA isoforms in U2OS cells. *miR34a* AS ref. refers to the full length transcript as defined by the 3'-RACE and primer walk assay. **D)** Analysis of coding potential of the *miR34a* asRNA transcript using the Coding-potential Calculator. **E)** RNAseq data from five fractionated cell lines in the ENCODE project showing the percentage of transcripts per million (TPM) for miR34a asRNA. MALAT1 (nuclear localization) and GAPDH (cytoplasmic localization) are included as fractionation controls. Points represent the mean and horizontal lines represent the standard deviation from two biological replicates.

A)



B)



704
705
706
707
708
709

Figure 2 Supplement 1: **A)** A UCSC genome browser illustration indicating the location of the promoter region cloned into the p1 construct including the conserved TP53-binding site. **B)** A representative picture of the p1 construct including forward (F) and reverse (R) primer locations and the renilla shRNA targeting site.

710
711
712
713
714
715

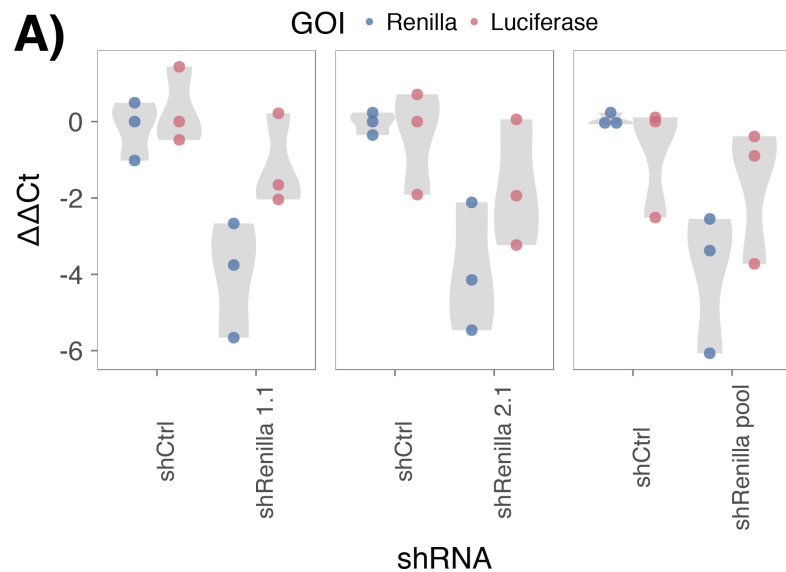
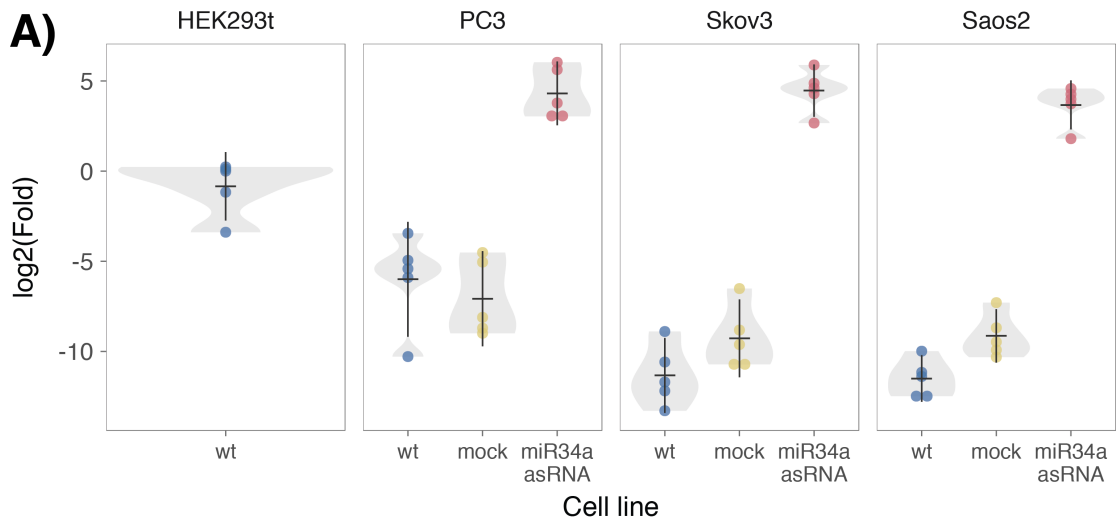
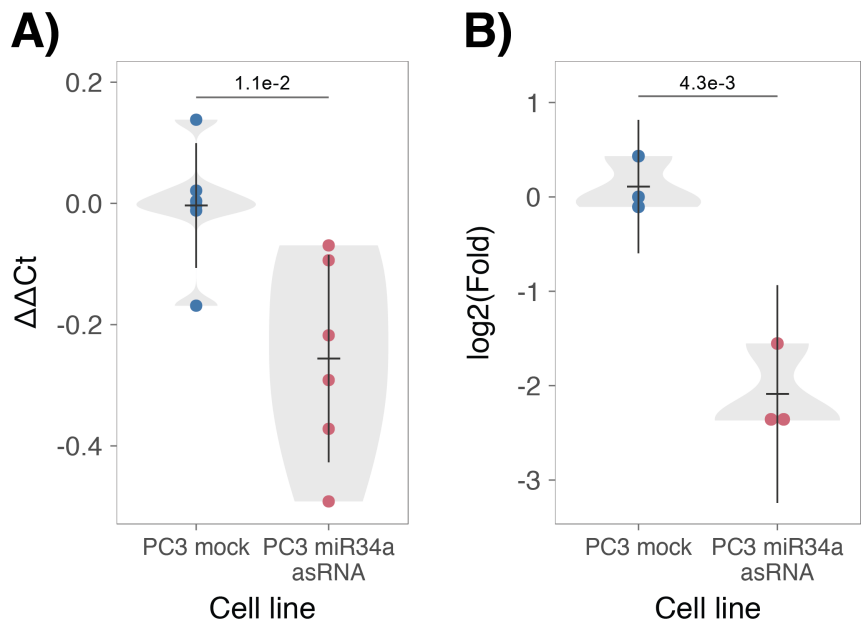


Figure 2 Supplement 2: A) HEK293t cells were co-transfected with the P1 construct and either shRenilla or shControl. Renilla and luciferase levels were measured with Q-PCR 48 hours after transfection. Individual points represent independent experiments with the gray shadow indicating the density of the points.



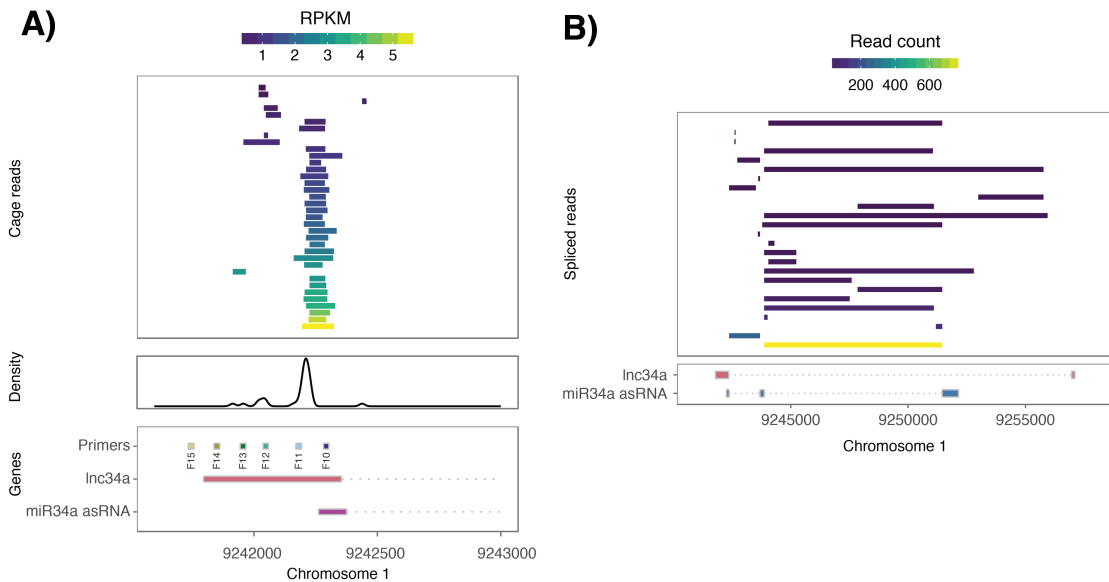
716
717
718
719
720

Figure 3 Supplement 1: A) Comparison of *miR34a* asRNA expression in HEK293T cells (high endogenous *miR34a* asRNA), and the wild-type (wt), mock, and *miR34a* asRNA over-expressing stable cell lines.



721
722

723 **Figure 3 Supplement 2:** CCND1 expression **(A)** and protein levels **(B)** in *miR34a* over-expressing PC3 stable cell lines.
724



725
726
727
728
729
730
731
732
733
734

Supplementary Figure 4: A) CAGE transcription start sites from 28 ENCODE cell lines which mapped between 200 base pairs upstream of the *lnc34a* start site and 200 base pairs upstream of the GENCODE annotated *miR34a* asRNA start site (top panel). The density of the CAGE reads (middle panel) and the transcription start regions for *lnc34a* and the annotated *miR34a* asRNA, as well as, primer positions from the primer walk assay (bottom panel) are also illustrated. B) Spliced reads from 36 ENCODE cell lines which had reads mapping to the *lnc34a/miR34a* asRNA locus (top panel) and the *lnc34a* and *miR34a* asRNA genes (bottom panel).

- 735
736 **References**
737
- 738 Agostini, M., P. Tucci, R. Killick, E. Candi, B. S. Sayan, P. Rivetti di Val Cervo, P.
739 Nicotera, F. McKeon, R. A. Knight, T. W. Mak and G. Melino (2011). "Neuronal
740 differentiation by TAp73 is mediated by microRNA-34a regulation of synaptic
741 protein targets." *Proc Natl Acad Sci U S A* **108**(52): 21093-21098. DOI:
742 10.1073/pnas.1112061109
743
- 744 Ahn, Y. H., D. L. Gibbons, D. Chakravarti, C. J. Creighton, Z. H. Rizvi, H. P. Adams,
745 A. Pertsemlidis, P. A. Gregory, J. A. Wright, G. J. Goodall, E. R. Flores and J. M.
746 Kurie (2012). "ZEB1 drives prometastatic actin cytoskeletal remodeling by
747 downregulating miR-34a expression." *J Clin Invest* **122**(9): 3170-3183. DOI:
748 10.1172/JCI63608
749
- 750 Allaire, J., Y. Xie, J. McPherson, J. Luraschi, K. Ushey, A. Atkins, H. Wickham, J.
751 Cheng and W. Chang (2017). rmarkdown: Dynamic Documents for R. R package
752 version 1.8. <https://CRAN.R-project.org/package=rmarkdown>
753
- 754 Amarzguioui, M., J. J. Rossi and D. Kim (2005). "Approaches for chemically
755 synthesized siRNA and vector-mediated RNAi." *FEBS Lett* **579**(26): 5974-5981.
756 DOI: 10.1016/j.febslet.2005.08.070
757
- 758 Arnold, J. B. (2017). ggthemes: Extra Themes, Scales and Geoms for 'ggplot2'. R
759 package version 3.4.0. <https://CRAN.R-project.org/package=ggthemes>
760
- 761 Ashouri, A., V. I. Sayin, J. Van den Eynden, S. X. Singh, T. Papagiannakopoulos and
762 E. Larsson (2016). "Pan-cancer transcriptomic analysis associates long non-coding
763 RNAs with key mutational driver events." *Nature Communications* **7**: 13197. DOI:
764 10.1038/ncomms13197
765
- 766 Balbin, O. A., R. Malik, S. M. Dhanasekaran, J. R. Prensner, X. Cao, Y. M. Wu, D.
767 Robinson, R. Wang, G. Chen, D. G. Beer, A. I. Nesvizhskii and A. M. Chinnaian
768 (2015). "The landscape of antisense gene expression in human cancers." *Genome Res*
769 **25**(7): 1068-1079. DOI: 10.1101/gr.180596.114
770
- 771 Chang, T. C., D. Yu, Y. S. Lee, E. A. Wentzel, D. E. Arking, K. M. West, C. V.
772 Dang, A. Thomas-Tikhonenko and J. T. Mendell (2008). "Widespread microRNA
773 repression by Myc contributes to tumorigenesis." *Nat Genet* **40**(1): 43-50. DOI:
774 10.1038/ng.2007.30
775
- 776 Chang, W. (2014). extrafont: Tools for using fonts. R package version 0.17.
777 <https://CRAN.R-project.org/package=extrafont>
778
- 779 Chen, J., M. Sun, W. J. Kent, X. Huang, H. Xie, W. Wang, G. Zhou, R. Z. Shi and J.
780 D. Rowley (2004). "Over 20% of human transcripts might form sense-antisense
781 pairs." *Nucleic Acids Res* **32**(16): 4812-4820. DOI: 10.1093/nar/gkh818
782
- 783 Cheng, J., L. Zhou, Q. F. Xie, H. Y. Xie, X. Y. Wei, F. Gao, C. Y. Xing, X. Xu, L. J.
784 Li and S. S. Zheng (2010). "The impact of miR-34a on protein output in

785 hepatocellular carcinoma HepG2 cells." Proteomics **10**(8): 1557-1572. DOI:
786 10.1002/pmic.200900646
787
788 Chim, C. S., K. Y. Wong, Y. Qi, F. Loong, W. L. Lam, L. G. Wong, D. Y. Jin, J. F.
789 Costello and R. Liang (2010). "Epigenetic inactivation of the miR-34a in
790 hematological malignancies." Carcinogenesis **31**(4): 745-750. DOI:
791 10.1093/carcin/bgq033
792
793 Cole, K. A., E. F. Attiyeh, Y. P. Mosse, M. J. Laquaglia, S. J. Diskin, G. M. Brodeur
794 and J. M. Maris (2008). "A functional screen identifies miR-34a as a candidate
795 neuroblastoma tumor suppressor gene." Mol Cancer Res **6**(5): 735-742. DOI:
796 10.1158/1541-7786.MCR-07-2102
797
798 Conley, A. B. and I. K. Jordan (2012). "Epigenetic regulation of human cis-natural
799 antisense transcripts." Nucleic Acids Res **40**(4): 1438-1445. DOI:
800 10.1093/nar/gkr1010
801
802 Consortium, E. P. (2012). "An integrated encyclopedia of DNA elements in the
803 human genome." Nature **489**(7414): 57-74. DOI: 10.1038/nature11247
804
805 Core, L. J., J. J. Waterfall and J. T. Lis (2008). "Nascent RNA sequencing reveals
806 widespread pausing and divergent initiation at human promoters." Science **322**(5909):
807 1845-1848. DOI: 10.1126/science.1162228
808
809 Derrien, T., R. Johnson, G. Bussotti, A. Tanzer, S. Djebali, H. Tilgner, G. Guernec,
810 D. Martin, A. Merkel, D. G. Knowles, J. Lagarde, L. Veeravalli, X. Ruan, Y. Ruan, T.
811 Lassmann, P. Carninci, J. B. Brown, L. Lipovich, J. M. Gonzalez, M. Thomas, C. A.
812 Davis, R. Shiekhattar, T. R. Gingeras, T. J. Hubbard, C. Notredame, J. Harrow and R.
813 Guigo (2012). "The GENCODE v7 catalog of human long noncoding RNAs: analysis
814 of their gene structure, evolution, and expression." Genome Res **22**(9): 1775-1789.
815 DOI: 10.1101/gr.132159.111
816
817 Ding, N., H. Wu, T. Tao and E. Peng (2017). "NEAT1 regulates cell proliferation and
818 apoptosis of ovarian cancer by miR-34a-5p/BCL2." Onco Targets Ther **10**: 4905-
819 4915. DOI: 10.2147/OTT.S142446
820
821 Djebali, S., C. A. Davis, A. Merkel, A. Dobin, T. Lassmann, A. Mortazavi, A. Tanzer,
822 J. Lagarde, W. Lin, F. Schlesinger, C. Xue, G. K. Marinov, J. Khatun, B. A. Williams,
823 C. Zaleski, J. Rozowsky, M. Roder, F. Kokocinski, R. F. Abdelhamid, T. Alioto, I.
824 Antoshechkin, M. T. Baer, N. S. Bar, P. Batut, K. Bell, I. Bell, S. Chakrabortty, X.
825 Chen, J. Chrast, J. Curado, T. Derrien, J. Drenkow, E. Dumais, J. Dumais, R.
826 Duttagupta, E. Falconnet, M. Fastuca, K. Fejes-Toth, P. Ferreira, S. Foissac, M. J.
827 Fullwood, H. Gao, D. Gonzalez, A. Gordon, H. Gunawardena, C. Howald, S. Jha, R.
828 Johnson, P. Kapranov, B. King, C. Kingswood, O. J. Luo, E. Park, K. Persaud, J. B.
829 Preall, P. Ribeca, B. Risk, D. Robyr, M. Sammeth, L. Schaffer, L. H. See, A. Shahab,
830 J. Skancke, A. M. Suzuki, H. Takahashi, H. Tilgner, D. Trout, N. Walters, H. Wang,
831 J. Wrobel, Y. Yu, X. Ruan, Y. Hayashizaki, J. Harrow, M. Gerstein, T. Hubbard, A.
832 Reymond, S. E. Antonarakis, G. Hannon, M. C. Giddings, Y. Ruan, B. Wold, P.
833 Carninci, R. Guigo and T. R. Gingeras (2012). "Landscape of transcription in human
834 cells." Nature **489**(7414): 101-108. DOI: 10.1038/nature11233

- 835
836 Gallardo, E., A. Navarro, N. Vinolas, R. M. Marrades, T. Diaz, B. Gel, A. Quera, E.
837 Bandres, J. Garcia-Foncillas, J. Ramirez and M. Monzo (2009). "miR-34a as a
838 prognostic marker of relapse in surgically resected non-small-cell lung cancer."
839 Carcinogenesis **30**(11): 1903-1909. DOI: 10.1093/carcin/bgp219
840
841 Hunten, S., M. Kaller, F. Drepper, S. Oeljeklaus, T. Bonfert, F. Erhard, A. Dueck, N.
842 Eichner, C. C. Friedel, G. Meister, R. Zimmer, B. Warscheid and H. Hermeking
843 (2015). "p53-Regulated Networks of Protein, mRNA, miRNA, and lncRNA
844 Expression Revealed by Integrated Pulsed Stable Isotope Labeling With Amino Acids
845 in Cell Culture (pSILAC) and Next Generation Sequencing (NGS) Analyses." Mol
846 Cell Proteomics **14**(10): 2609-2629. DOI: 10.1074/mcp.M115.050237
847
848 International Human Genome Sequencing, C. (2004). "Finishing the euchromatic
849 sequence of the human genome." Nature **431**(7011): 931-945. DOI:
850 10.1038/nature03001
851
852 Johnsson, P., A. Ackley, L. Vidarsdottir, W. O. Lui, M. Corcoran, D. Grander and K.
853 V. Morris (2013). "A pseudogene long-noncoding-RNA network regulates PTEN
854 transcription and translation in human cells." Nat Struct Mol Biol **20**(4): 440-446.
855 DOI: 10.1038/nsmb.2516
856
857 Katayama, S., Y. Tomaru, T. Kasukawa, K. Waki, M. Nakanishi, M. Nakamura, H.
858 Nishida, C. C. Yap, M. Suzuki, J. Kawai, H. Suzuki, P. Carninci, Y. Hayashizaki, C.
859 Wells, M. Frith, T. Ravasi, K. C. Pang, J. Hallinan, J. Mattick, D. A. Hume, L.
860 Lipovich, S. Batalov, P. G. Engstrom, Y. Mizuno, M. A. Faghihi, A. Sandelin, A. M.
861 Chalk, S. Mottagui-Tabar, Z. Liang, B. Lenhard, C. Wahlestedt, R. G. E. R. Group, G.
862 Genome Science and F. Consortium (2005). "Antisense transcription in the
863 mammalian transcriptome." Science **309**(5740): 1564-1566. DOI:
864 10.1126/science.1112009
865
866 Kent, W. J., C. W. Sugnet, T. S. Furey, K. M. Roskin, T. H. Pringle, A. M. Zahler and
867 D. Haussler (2002). "The human genome browser at UCSC." Genome Res **12**(6):
868 996-1006. DOI: 10.1101/gr.229102. Article published online before print in May
869 2002
870
871 Kim, K. H., H. J. Kim and T. R. Lee (2017). "Epidermal long non-coding RNAs are
872 regulated by ultraviolet irradiation." Gene **637**: 196-202. DOI:
873 10.1016/j.gene.2017.09.043
874
875 Kong, L., Y. Zhang, Z. Q. Ye, X. Q. Liu, S. Q. Zhao, L. Wei and G. Gao (2007).
876 "CPC: assess the protein-coding potential of transcripts using sequence features and
877 support vector machine." Nucleic Acids Res **35**(Web Server issue): W345-349. DOI:
878 10.1093/nar/gkm391
879
880 Lal, A., M. P. Thomas, G. Altschuler, F. Navarro, E. O'Day, X. L. Li, C. Concepcion,
881 Y. C. Han, J. Thiery, D. K. Rajani, A. Deutsch, O. Hofmann, A. Ventura, W. Hide
882 and J. Lieberman (2011). "Capture of microRNA-bound mRNAs identifies the tumor
883 suppressor miR-34a as a regulator of growth factor signaling." PLoS Genet **7**(11):
884 e1002363. DOI: 10.1371/journal.pgen.1002363

- 885
886 Leveille, N., C. A. Melo, K. Rooijers, A. Diaz-Lagares, S. A. Melo, G. Korkmaz, R.
887 Lopes, F. Akbari Moqadam, A. R. Maia, P. J. Wijchers, G. Geeven, M. L. den Boer,
888 R. Kalluri, W. de Laat, M. Esteller and R. Agami (2015). "Genome-wide profiling of
889 p53-regulated enhancer RNAs uncovers a subset of enhancers controlled by a
890 lncRNA." Nature Communications **6**: 6520. DOI: 10.1038/ncomms7520
891
892 Liu, C., K. Kelnar, B. Liu, X. Chen, T. Calhoun-Davis, H. Li, L. Patrawala, H. Yan,
893 C. Jeter, S. Honorio, J. F. Wiggins, A. G. Bader, R. Fagin, D. Brown and D. G. Tang
894 (2011). "The microRNA miR-34a inhibits prostate cancer stem cells and metastasis
895 by directly repressing CD44." Nat Med **17**(2): 211-215. DOI: 10.1038/nm.2284
896
897 Memczak, S., M. Jens, A. Elefsinioti, F. Torti, J. Krueger, A. Rybak, L. Maier, S. D.
898 Mackowiak, L. H. Gregersen, M. Munschauer, A. Loewer, U. Ziebold, M. Landthaler,
899 C. Kocks, F. le Noble and N. Rajewsky (2013). "Circular RNAs are a large class of
900 animal RNAs with regulatory potency." Nature **495**(7441): 333-338. DOI:
901 10.1038/nature11928
902
903 Neil, H., C. Malabat, Y. d'Aubenton-Carafa, Z. Xu, L. M. Steinmetz and A. Jacquier
904 (2009). "Widespread bidirectional promoters are the major source of cryptic
905 transcripts in yeast." Nature **457**(7232): 1038-1042. DOI: 10.1038/nature07747
906
907 O'Leary, N. A., M. W. Wright, J. R. Brister, S. Ciuffo, D. Haddad, R. McVeigh, B.
908 Rajput, B. Robbertse, B. Smith-White, D. Ako-Adjei, A. Astashyn, A. Badretdin, Y.
909 Bao, O. Blinkova, V. Brover, V. Chetvernin, J. Choi, E. Cox, O. Ermolaeva, C. M.
910 Farrell, T. Goldfarb, T. Gupta, D. Haft, E. Hatcher, W. Hlavina, V. S. Joardar, V. K.
911 Kodali, W. Li, D. Maglott, P. Masterson, K. M. McGarvey, M. R. Murphy, K.
912 O'Neill, S. Pujar, S. H. Rangwala, D. Rausch, L. D. Riddick, C. Schoch, A. Shkeda,
913 S. S. Storz, H. Sun, F. Thibaud-Nissen, I. Tolstoy, R. E. Tully, A. R. Vatsan, C.
914 Wallin, D. Webb, W. Wu, M. J. Landrum, A. Kimchi, T. Tatusova, M. DiCuccio, P.
915 Kitts, T. D. Murphy and K. D. Pruitt (2016). "Reference sequence (RefSeq) database
916 at NCBI: current status, taxonomic expansion, and functional annotation." Nucleic
917 Acids Res **44**(D1): D733-745. DOI: 10.1093/nar/gkv1189
918
919 Ozsolak, F., P. Kapranov, S. Foissac, S. W. Kim, E. Fishilevich, A. P. Monaghan, B.
920 John and P. M. Milos (2010). "Comprehensive polyadenylation site maps in yeast and
921 human reveal pervasive alternative polyadenylation." Cell **143**(6): 1018-1029. DOI:
922 10.1016/j.cell.2010.11.020
923
924 Pelechano, V. and L. M. Steinmetz (2013). "Gene regulation by antisense
925 transcription." Nat Rev Genet **14**(12): 880-893. DOI: 10.1038/nrg3594
926
927 Polson, A., E. Durrett and D. Reisman (2011). "A bidirectional promoter reporter
928 vector for the analysis of the p53/WDR79 dual regulatory element." Plasmid **66**(3):
929 169-179. DOI: 10.1016/j.plasmid.2011.08.004
930
931 Rashi-Elkeles, S., H. J. Warnatz, R. Elkon, A. Kupershtain, Y. Chobod, A. Paz, V.
932 Amstislavskiy, M. Sultan, H. Safer, W. Nietfeld, H. Lehrach, R. Shamir, M. L. Yaspo
933 and Y. Shiloh (2014). "Parallel profiling of the transcriptome, cistrome, and

- 934 epigenome in the cellular response to ionizing radiation." Sci Signal **7**(325): rs3. DOI:
935 10.1126/scisignal.2005032
- 936
- 937 Raver-Shapira, N., E. Marciano, E. Meiri, Y. Spector, N. Rosenfeld, N. Moskovits, Z.
938 Bentwich and M. Oren (2007). "Transcriptional activation of miR-34a contributes to
939 p53-mediated apoptosis." Mol Cell **26**(5): 731-743. DOI:
940 10.1016/j.molcel.2007.05.017
- 941
- 942 Rinn, J. L., M. Kertesz, J. K. Wang, S. L. Squazzo, X. Xu, S. A. Brugmann, L. H.
943 Goodnough, J. A. Helms, P. J. Farnham, E. Segal and H. Y. Chang (2007).
944 "Functional demarcation of active and silent chromatin domains in human HOX loci
945 by noncoding RNAs." Cell **129**(7): 1311-1323. DOI: 10.1016/j.cell.2007.05.022
- 946
- 947 Rokavec, M., M. G. Oner, H. Li, R. Jackstadt, L. Jiang, D. Lodygin, M. Kaller, D.
948 Horst, P. K. Ziegler, S. Schwitalla, J. Slotta-Huspenina, F. G. Bader, F. R. Greten and
949 H. Hermeking (2015). "Corrigendum. IL-6R/STAT3/miR-34a feedback loop
950 promotes EMT-mediated colorectal cancer invasion and metastasis." J Clin Invest
951 **125**(3): 1362. DOI: 10.1172/JCI81340
- 952
- 953 Schneider, C. A., W. S. Rasband and K. W. Eliceiri (2012). "NIH Image to ImageJ:
954 25 years of image analysis." Nat Methods **9**(7): 671-675.
- 955
- 956 Seila, A. C., J. M. Calabrese, S. S. Levine, G. W. Yeo, P. B. Rahl, R. A. Flynn, R. A.
957 Young and P. A. Sharp (2008). "Divergent transcription from active promoters."
958 Science **322**(5909): 1849-1851. DOI: 10.1126/science.1162253
- 959
- 960 Serviss, J. T. (2017). miR34AasRNAProject.
961 https://github.com/GranderLab/miR34a_asRNA_project
- 962
- 963 Sigova, A. A., A. C. Mullen, B. Molinie, S. Gupta, D. A. Orlando, M. G. Guenther,
964 A. E. Almada, C. Lin, P. A. Sharp, C. C. Giallourakis and R. A. Young (2013).
965 "Divergent transcription of long noncoding RNA/mRNA gene pairs in embryonic
966 stem cells." Proc Natl Acad Sci U S A **110**(8): 2876-2881. DOI:
967 10.1073/pnas.1221904110
- 968
- 969 Slabakova, E., Z. Culig, J. Remsik and K. Soucek (2017). "Alternative mechanisms of
970 miR-34a regulation in cancer." Cell Death Dis **8**(10): e3100. DOI:
971 10.1038/cddis.2017.495
- 972
- 973 Spizzo, R., M. I. Almeida, A. Colombatti and G. A. Calin (2012). "Long non-coding
974 RNAs and cancer: a new frontier of translational research?" Oncogene **31**(43): 4577-
975 4587. DOI: 10.1038/onc.2011.621
- 976
- 977 Stahlhut, C. and F. J. Slack (2015). "Combinatorial Action of MicroRNAs let-7 and
978 miR-34 Effectively Synergizes with Erlotinib to Suppress Non-small Cell Lung
979 Cancer Cell Proliferation." Cell Cycle **14**(13): 2171-2180. DOI:
980 10.1080/15384101.2014.1003008
- 981
- 982 Struhl, K. (2007). "Transcriptional noise and the fidelity of initiation by RNA
983 polymerase II." Nat Struct Mol Biol **14**(2): 103-105. DOI: 10.1038/nsmb0207-103

- 984
985 Su, X., D. Chakravarti, M. S. Cho, L. Liu, Y. J. Gi, Y. L. Lin, M. L. Leung, A. El-
986 Naggar, C. J. Creighton, M. B. Suraokar, I. Wistuba and E. R. Flores (2010). "TAp63
987 suppresses metastasis through coordinate regulation of Dicer and miRNAs." *Nature*
988 **467**(7318): 986-990. DOI: 10.1038/nature09459
989
990 Sun, F., H. Fu, Q. Liu, Y. Tie, J. Zhu, R. Xing, Z. Sun and X. Zheng (2008).
991 "Downregulation of CCND1 and CDK6 by miR-34a induces cell cycle arrest." *FEBS*
992 *Lett* **582**(10): 1564-1568. DOI: 10.1016/j.febslet.2008.03.057
993
994 Team, R. C. (2017). "R: A Language and Environment for Statistical Computing."
995 from <https://www.R-project.org/>.
996
997 Turner, A. M., A. M. Ackley, M. A. Matrone and K. V. Morris (2012).
998 "Characterization of an HIV-targeted transcriptional gene-silencing RNA in primary
999 cells." *Hum Gene Ther* **23**(5): 473-483. DOI: 10.1089/hum.2011.165
1000
1001 Vanhee-Brossollet, C. and C. Vaquero (1998). "Do natural antisense transcripts make
1002 sense in eukaryotes?" *Gene* **211**(1): 1-9.
1003
1004 Vogt, M., J. Mundig, M. Gruner, S. T. Liffers, B. Verdoodt, J. Hauk, L.
1005 Steinstraesser, A. Tannapfel and H. Hermeking (2011). "Frequent concomitant
1006 inactivation of miR-34a and miR-34b/c by CpG methylation in colorectal, pancreatic,
1007 mammary, ovarian, urothelial, and renal cell carcinomas and soft tissue sarcomas."
1008 *Virchows Arch* **458**(3): 313-322. DOI: 10.1007/s00428-010-1030-5
1009
1010 Wagner, E. G. and R. W. Simons (1994). "Antisense RNA control in bacteria, phages,
1011 and plasmids." *Annu Rev Microbiol* **48**: 713-742. DOI:
1012 10.1146/annurev.mi.48.100194.003433
1013
1014 Wang, L., P. Bu, Y. Ai, T. Srinivasan, H. J. Chen, K. Xiang, S. M. Lipkin and X.
1015 Shen (2016). "A long non-coding RNA targets microRNA miR-34a to regulate colon
1016 cancer stem cell asymmetric division." *eLife* **5**. DOI: 10.7554/eLife.14620
1017
1018 Wang, L., H. J. Park, S. Dasari, S. Wang, J. P. Kocher and W. Li (2013). "CPAT:
1019 Coding-Potential Assessment Tool using an alignment-free logistic regression
1020 model." *Nucleic Acids Res* **41**(6): e74. DOI: 10.1093/nar/gkt006
1021
1022 Wang, X., J. Li, K. Dong, F. Lin, M. Long, Y. Ouyang, J. Wei, X. Chen, Y. Weng, T.
1023 He and H. Zhang (2015). "Tumor suppressor miR-34a targets PD-L1 and functions as
1024 a potential immunotherapeutic target in acute myeloid leukemia." *Cell Signal* **27**(3):
1025 443-452. DOI: 10.1016/j.cellsig.2014.12.003
1026
1027 Wickham, H. (2016). gtable: Arrange 'Grobs' in Tables. R package version 0.2.0.
1028 <https://CRAN.R-project.org/package=gtable>
1029
1030 Wickham, H. (2017). scales: Scale Functions for Visualization. R package version
1031 0.5.0. <https://CRAN.R-project.org/package=scales>
1032

- 1033 Wickham, H. (2017). tidyverse: Easily Install and Load the 'Tidyverse'. R package
1034 version 1.2.1. <https://CRAN.R-project.org/package=tidyverse>
- 1035
- 1036 Wickham, L. H. a. H. (2017). rlang: Functions for Base Types and Core R and
1037 'Tidyverse' Features. R package version 0.1.4. <https://CRAN.R->
1038 [project.org/package=rlang](https://CRAN.R-project.org/package=rlang)
- 1039
- 1040 Wickham, S. M. B. a. H. (2014). magrittr: A Forward-Pipe Operator for R. R package
1041 version 1.5. <https://CRAN.R-project.org/package=magrittr>
- 1042
- 1043 Wilkins, D. ggenes: Draw Gene Arrow Maps in 'ggplot2'. R package version
1044 0.2.0.9003. <https://github.com/wilcox/ggenes>
- 1045
- 1046 Xiao, N. (2017). liftr: Containerize R Markdown Documents. R package version 0.7.
<https://CRAN.R-project.org/package=liftr>
- 1048
- 1049 Xie, Y. (2017). knitr: A General-Purpose Package for Dynamic Report Generation in
1050 R. R package version 1.17. <https://yihui.name/knitr/>
- 1051
- 1052 Yang, P., Q. J. Li, Y. Feng, Y. Zhang, G. J. Markowitz, S. Ning, Y. Deng, J. Zhao, S.
1053 Jiang, Y. Yuan, H. Y. Wang, S. Q. Cheng, D. Xie and X. F. Wang (2012). "TGF-beta-
1054 miR-34a-CCL22 signaling-induced Treg cell recruitment promotes venous metastases
1055 of HBV-positive hepatocellular carcinoma." *Cancer Cell* **22**(3): 291-303. DOI:
1056 10.1016/j.ccr.2012.07.023
- 1057
- 1058 Yap, K. L., S. Li, A. M. Munoz-Cabello, S. Raguz, L. Zeng, S. Mujtaba, J. Gil, M. J.
1059 Walsh and M. M. Zhou (2010). "Molecular interplay of the noncoding RNA ANRIL
1060 and methylated histone H3 lysine 27 by polycomb CBX7 in transcriptional silencing
1061 of INK4a." *Mol Cell* **38**(5): 662-674. DOI: 10.1016/j.molcel.2010.03.021
- 1062
- 1063 Zenz, T., J. Mohr, E. Eldering, A. P. Kater, A. Buhler, D. Kienle, D. Winkler, J.
1064 Durig, M. H. van Oers, D. Mertens, H. Dohner and S. Stilgenbauer (2009). "miR-34a
1065 as part of the resistance network in chronic lymphocytic leukemia." *Blood* **113**(16):
1066 3801-3808. DOI: 10.1182/blood-2008-08-172254
- 1067
- 1068